Structure-guided design of a novel class of benzyl-sulfonate inhibitors for influenza virus neuraminidase

Dimitris Platis, Brian J Smith, Trevor Huyton, Nikolaos E Labrou

Biochemical Journal Immediate Publication. Published on 16 Jun 2006 as manuscript BJ20060447

Structure-guided design of a novel class of benzyl-sulphonate inhibitors for influenza virus neuraminidase.

Dimitris Platis[1], Brian J. Smith[2], Trevor Huyton[2] and Nikolaos E. Labrou[1,*]

[1]Laboratory of Enzyme Technology, Department of Agricultural Biotechnology, Agricultural University of Athens, Iera Odos 75, 11855-Athens, Greece,

[2] The Walter & Eliza Hall Institute of Medical Research, 1G Royal Parade, Parkville Victoria 3050, Australia.

[1] To whom correspondence should be addressed

Email: lambrou@aua.gr,

Fax: +30 210 5294308.

ABSTRACT

Influenza neuraminidase (NA) is an antiviral target of high pharmaceutical interest because of its essential role in cleaving sialic acid residues from cell surface glycoproteins and facilitating release of virions from infected cells. The present work describes the use of structural information in the progressive design from a lead binding ion, a sulphate, to a potent submicromolor inhibitor (K_i 0.13 μM). Structural information derived from the X-ray structure of a NA complexed with several sulphate ions, in combination with data derived by affinity labelling and molecular modelling studies, was used to guide design of potent sulphonic acid-based inhibitors. These inhibitors are structural fragments of polysulphonate triazine dye Cibacron Blue 3GA (CB3GA), and represent novel lead scaffolds for designing non-carbohydrate inhibitors for influenza neuraminidases.

Running title: Structure-guided inhibitors for neuraminidase

Key words: neuraminidase inhibitors; influenza; Structure-guided design; Cibacron Blue 3GA.

Abbreviations: CB3GA, Cibacron Blue 3GA; HPLC, high-performance liquid chromatography; NA, neuraminidase; SBS, sulphate binding subsite.

INTRODUCTION

Influenza is a highly contagious, acute viral respiratory disease which occurs seasonally in most parts of the world. Epidemics with high attack rates, a short incubation period, and rapid progression of the disease through the population are characteristic [1]. The hallmark of influenza is this epidemicity. The public health impact of influenza is dramatic. Greater than 10,000 deaths occurred in each of 7 U.S. epidemics in the period 1977-1988, and greater than 40,000 deaths occurred during two of these epidemics. The 1918 "Spanish Flu" killed more than 500,000 people in the United States, and 20-50 million people worldwide [2]. Vaccination remains the primary method for prevention of influenza, but vaccine strains must be continually updated and their protective efficacy is limited in patients beyond 65 years of age, the major target group [3]. An alternative lies in antiviral drugs. Influenza neuraminidase (NA) has been proven as a valid therapeutic target for antiviral drugs due to its essential role in the viral replication cycle [4]. NA is thought to enhance viral mobility *via* hydrolysis of the α-(2,3) or α-(2,6) glycosidic linkage between a terminal sialic acid (Neu5Ac) residue and its adjacent carbohydrate moiety on the host receptor. These molecules with terminal Neu5Ac are also the target receptors for the viral hemagglutinin (HA) [5], the major surface glycoprotein on the viral particle surface. NA destroys these HA receptors, allowing progeny virus particles, budding from infected cell surfaces, to be released [6,7].

Neuraminidase is a tetramer of identical, 60 kDa, glycosylated subunits. X-ray diffraction studies revealed a polypeptide fold of β sheets, six in total, arranged like the blades of a propeller. Each sheet is composed of four antiparallel strands and has the topology of the letter 'W'. The active site is centrally located on the neuraminidase subunit and lies on the propeller axis at the N-terminal ends of the first β strand of each sheet [4].

The discovery of inhibitors of NA for the treatment of influenza infection has been an active area of research [8-13]. NA inhibitors are a class of anti-influenza drugs used for both prophylaxis and treatment of influenza virus infections. Modern approaches for finding new leads for therapeutic targets are increasingly based on three-dimensional information about receptors [14,15]. The ready availability of crystal

structures of inhibitor/NA complexes has enabled a detailed analysis of the structural basis for potent inhibition [16,17]. For example, with the aid of the X-ray crystal structure of NA complexed with sialic acid or 2,3-dehydro-sialic acid, the nanomolar inhibitors zanamivir and oseltamivir were designed as enzyme substrate mimics [17-19]. These compounds display high potency and specificity both *in vitro* and *in vivo* and are effective prophylactics. Both drugs were introduced into clinical practice in various parts of the world during 1999–2002, and share similar potency and specificity for all subtypes of influenza A and B virus NA [18,19].

The development of neuraminidase inhibitor-resistant influenza virus strains is a serious concern and there is an urgent need for research on newer anti-neuraminidase agents [1,2,9]. In the present report we describe a structure-guided approach to the design of a new class of non-carbohydrate benzyl-sulphonate inhibitors, and examine their binding features in the active-site pocket of influenza NA. Non-carbohydrate inhibitors give the advantages of high chemical and metabolic stability

MATERIALS AND METHODS

Materials.

Cyanuric chloride (1,3,5-sym-trichlorotriazine), Cibacron Blue 3GA (CB3GA), 1-amino-4-bromo-2-methyl-4a,9a-dihydroanthracene-9,10-dione and all other reagents and chemicals were of analytical grade and obtained from Sigma-Aldrich Co (USA). Crystalline bovine serum albumin (fraction V) was obtained from Boehringer Mannheim, Germany.

Expression and purification of NA.

Expression of A/Beijing/262/95 H1N1 influenza NA was accomplished in expressSF+® insect cells, using the Baculovirus Expression Vector system [20]. Purification of NA was carried out as described in [20].

Synthesis and purification of CB3GA and other analogues.

Purification of CB3GA.

Solid commercial dye (purity 61.3 %, w/w) was purified to homogeneity in two stages according the procedure of Labrou & Clonis [21], as follows: 100 mg dye was

dissolved in deionised water (20 ml) by stirring at room temperature. The solution was extracted twice with diethyl ether (2 x 20 ml), the aqueous phase concentrated (approx. threefold) on a rotary evaporator and the dye precipitated by addition of cold acetone (60 ml). The precipitate was filtered through Whatman filter paper and dried overnight under reduced pressure. Dried dye was dissolved in water/methanol (5 ml, 50/50 v/v) and filtered through a 0.45-ìm-pore-size cellulose membrane filter (Millipore). The dye solution was applied on a lipophilic Sephadex LH-20 column (2.5 x 30 cm) previously equilibrated in water/methanol (50/50 v/v). The column was developed isocratically at a flow rate of 0.1 ml min^{-1} cm^{-1}. Fractions (5 ml) were collected and analyzed by TLC and those with the pure dye were pooled, concentrated by 60 % on a rotary evaporator under reduced pressure, before the product was lyophilized and stored desiccated at 4°C.

Analysis of pure dye was performed by TLC and HPLC, whereas dye concentration was determined spectrophotometrically at 620 nm using a molar absorption coefficient of 12.6 l $mmol^{-1}$ cm^{-1} [21]. Ascending TLC was performed on precoated plastic sheets with silica gel 60 (0.2 mm; Merck) using solvent system butanol-1/propanol-2/ethylacetate/water (2/4/1/3). HPLC analysis was carried out on a C18 reverse phase S5 ODS2 Spherisorb silica column (250 mm x 4.6 mm I.D.). The starting solvent system composed of 80% (v/v) methanol and 20% (v/v) water containing 0.1% (w/v) *N*-acetyltrimethylammonium bromide.

The hydrolyzed analogue of 1-Amino-4-[3-(4,6-dichlorotriazin-2-ylamino)-4-sulphophenylamino]anthraquinone-2-sulphonic acid was prepared by incubating in 0.1 M Na_2CO_3 at 25 °C for 1h as previously described [22]. Purification of the analogue was achieved by preparative TLC on silica gel 60 plates, using the solvent system butanol-1/propanol-2/ethylacetate/water (2/4/1/3). The blue band was scraped from the plate, and the product was eluted from silica with water. 1-amino-4-[(4-amino-3-methylphenyl)amino]-2-methyl-4a,9a-dihydroanthracene-9,10-dione was synthesized as described previously [22]. All dyes were found to be at least 98 % pure.

Synthesis of azido-CB3GA.

Azido-CB3GA was synthesised by diazotization of the anthraquinone amino group of CB3GA using the $NaNO_2$/HCl system following by nucleophilic displacement of the diazotized intermediate with NaN_3, as following: to a cooled and stirred solution of CB3GA (20 mg) in 1.5 ml of HCl (3M), a solution of sodium nitrite (10 mg in 0.2 ml of water) was added drop wise. The reaction mixture was kept cold by adding crushed ice and was continuously stirred. Immediately following, a solution of sodium azide (12 mg in 0.5 ml water) was gradually added to the vigorously stirred mixture. Stirring and cooling of the solution in an ice bath was continued for 2 h. Purification of azido-CB3GA was achieved by preparative TLC on silica gel 60 plates using the solvent system propanol/AcOH/H_2O (4/1/1). The red band was scraped from the plate, and the product was eluted from silica with water. The purity of the product was confirmed by HPLC. HPLC analysis was effected on a C18 reverse phase S5 ODS2 Spherisorb silica column (250 mm x 4.6 mm I.D.). The starting solvent system composed of 80% (v/v) methanol and 20% (v/v) water containing 0.1% (w/v) *N*-acetyltrimethylammonium bromide. Azido-CB3GA was found to be at least 98.4% pure.

Assay of enzyme activity and protein.

Enzyme assays were performed at pH 5.9 at 37°C according to the published method [23] using sialyl-lactose as substrate. Observed reaction velocities were corrected for spontaneous reaction rates where necessary. All initial velocities were determined in triplicate in buffers equilibrated at constant temperature. Turnover numbers were calculated on the basis of one active site per subunit. Protein concentration was determined by the method of Bradford [24] using bovine serum albumin (fraction V) as standard. Kinetic inhibition studies were carried out using sialyl-lactose as substrate at pH 5.9 at 37°C. No significant interference was observed from the inhibitors. Kinetic constants were deduced from Dixon's plot using the computer program GraFit (Erithacus Software Ltd., Leatherbarrow, 1998).

Difference spectroscopy.

Difference spectral titrations were performed on a Perkin-Elmer Lamda16 double beam double monochromator UV-VIS spectrophotometer at 37°C. Enzyme solution (1 ml; 10.5 μM in 20 mM potassium phosphate, pH 5.9) and enzyme solvent (1 ml; 20

mM potassium phosphate, pH 5.9) were placed in the sample and reference black-wall silica cuvettes (10 mm path length), respectively, and the baseline difference spectrum was recorded in the range 700-500 nm. Identical volumes (2-5µl) of dye solutions (0.5 mM) were added to both cuvettes and the difference spectra recorded after each addition. The difference absorption at λ_{max} was measured relative to a zero-absorbance reference area at 750 nm. The data were analyzed using the following equation [25]:

$$\Delta A = \frac{\Delta A_{max}[ligand]}{K_D + [ligand]} \qquad \text{equation 1}$$

where ΔA is the difference absorption at λ_{max} after each addition of dye-ligand, and ΔA_{max} is the maximum difference absorption at λ_{max} at saturated concentration of dye. The data were fitted to equation 1 using non-linear fitting using the computer program GraFit (Erithacus Software Ltd., Leatherbarrow, 1998).

Synthesis of triazine-based sulphonate analogues.

The synthesis was carried out as described in [26,27] with the following modifications: cyanuric chloride (1 mmol) was dissolved in 20 ml of ice-cold acetone:water (2:1) and added slowly to a solution of o-aminobenzenesulphonic acid (1 mmol, 20 ml ice-cold acetone:water, 2:1) over a period of 20 min under constant stirring. During the course of the reaction the pH was maintained at 6-7 by addition of 0.5 M $NaHCO_3$ and the temperature at 0-4°C. The progress of the reaction was monitored by thin layer chromatography (silica, chloroform/methanol/acetic acid, 8/4/0.5, v/v) until no cyanuric acid was detectable (after about 2 hours). On completion, 1mmol of o-aminobenzenesulphonic acid was added to the reaction and the mixture was heated to 40-50°C for 24 hours. The reaction was monitored by thin layer chromatography (silica, chloroform/methanol/acetic acid, 8/4/0.5, v/v). During the course of the reaction the pH was maintained at 6-7 by addition of 0.5 M $NaHCO_3$. On completion, the reaction was run on silica gel plates (20 x 20 cm) (solvent: chloroform/methanol/acetic acid, 8/4/0.5, v/v). The band corresponding to the bis-substituted triazine product was identified under UV and excised. The bis-substituted product was eluted from silica by subsequent resuspension in a mixture of

acetone:water (1:1) (5 ml x 3 times), the acetone removed by evaporation and the remaining liquid by lyophilization. The pure product (purity >95%) was subjected to MS analysis. The same procedure was followed for the synthesis of other bis-substituted triazine derivatives.

Reaction of azido-CB3GA with NA.

Recombinant NA (1 unit) was incubated at 4 °C in the dark with azido-CB3GA (20 μM) in 20 mM potassium phosphate buffer, pH 5.9. The solution (200 μl) was placed 2 cm in front of a UV lamp and irradiated. After various times of irradiation, an aliquot was diluted 10-fold with buffer and residual enzyme activity was determined. When Neu5Ac (1 mM) was tested for its ability to protect against inactivation, it was preincubated with the enzyme for 10 min prior to the addition of azido-CB3GA.

Stoichiometry of azido-CB3GA binding to NA.

Recombinant NA in 0.1 M potassium phosphate buffer, pH 6, was inactivated with azido-CB3GA at 4°C. The dye-inactivated enzyme was separated from the free dye by ultrafiltration (in an Amicon stirred cell 8050 carrying a Diaflo YM10 ultrafiltration membrane; cut-off 10 kDa) after extensive washing with distilled water. Further separation was achieved by gel-filtration chromatography by applying the inactive dye-enzyme complex to a Sephadex G-25 column (9 cm x 1.6 cm) equilibrated with water, and collecting fractions (0.5 ml) at a flow rate of 10 ml/h. The solution with dye-inactivated NA was then lyophilized and stored at –20 ºC. The lyophilized enzyme covalent complex was dissolved in 8 M urea, and the absorbance was determined spectrophotometrically at 520 nm using a molar extinction coefficient of 9.5 L/cm·mmol which was determined in 8 M urea. The protein concentration was determined by the method of Lowry [27]; no dye interference was observed in protein determinations.

Chymotryptic digestion of the azido-CB3GA covalent complex and peptide purification using high performance liquid chromatography.

Lyophilized neraminidase-azido-CB3GA covalent complex (100 μg) was dissolved in Hepes/NaOH buffer, (0.1 M, pH 7.0, 1 ml) and denatured by the addition of solid urea to yield 8 M solution. The denatured enzyme was treated by DTT (10 mM, 25°C, 1 h)

and N-ethyl-maleimide was added to a final concentration of 15 mM, and the solution incubated for 30 min at room temperature. The enzyme was then dialyzed against 0.1 M ammonium bicarbonate buffer, pH 8.3. The enzyme was digested by addition of 10 μg of chymotrypsin. The digestion was allowed to continue overnight at 30 ºC before the mixture was lyophilized and stored dry at –20 ºC. Separation of the resulting peptides was achieved on a C18 reverse phase S5 ODS2 Spherisorb silica column (250 mm x 4.6 mm I.D.). Analysis was effected with a H_2O/acetonitrile linear gradient containing 0.1% trifluoroacetic acid (0-80% acetonitrile during 80 min) at a flow rate 0.5 ml/min. Fractions of 0.5 ml were collected. The eluents were monitored at both 220 nm and 520 nm.

Molecular docking

The complex of NA with sulphate ions (PDB code 2B8H) was crystallized from buffer with ammonium sulphate [29]. This structure was prepared for docking by removing all crystallographic water molecules, solvent molecules and ions, and adding hydrogen atoms to fulfil unsatisfied valencies using the Sybyl program [30]. The positions of the hydrogen atoms was adjusted manually to ensure correct hydrogen-bonding patterns, then energy minimized until the maximum gradient was less than 0.2 kJ mol^{-1} $Å^{-1}$(with protein atoms held fixed). All-atom Kollman charges were assigned to protein atoms. Ionizable amino acids were modelled in their ionized state, with the exception of D151 that was neutral. The ligand was constructed manually, minimized, and Gasteiger charges assigned using the Sybyl program [30].

The DOCK [31] suite of programs was employed for predicting the geometry of the ligand bound to the protein. Electrostatic and van der Waals energies were evaluated on a grid [32] with a 0.3 Å spacing in the region spanning all residues within 12 Å of the active-site aspartate D151. A distance-dependent dielectric ($\varepsilon = 4r$) and an energy cut-off distance of 10 Å were used in evaluating the interaction energy between protein and ligand. The position of the sulphate-sulphur atoms in the X-ray crystal structure was used to define the docking spheres; matching of sphere centres with ligand sulphur atoms used a maximum distance tolerance of 0.5 Å. Ligand conformational flexibility was explored through torsion angle sampling and

minimization. The highest-ranked docked conformation was subjected to energy minimization in Sybyl [30] with all protein atoms held fixed.

RESULTS & DISCUSSION

Structure-guided lead ligand design.

Analysis of the crystal structure of whale N9 NA (PDB code 2B8H) [29], determined in sulphate buffer, revealed that four sulphate ions are located at well defined positions with sulphur atoms 6.0 - 7.6 Å apart (Figure 1A). One of them is located (sulphate binding subsite 1, SBS1) in the position usually occupied by the substrate's carboxylate moiety and forms ionic interactions with the side chain guanidinium groups of the arginine residues 119, 294 and 372 (numbering according to Figure 1B). One of the oxygen atoms of this sulphate anion also comes in close contact (~3.2 Å) with a carboxylate oxygen atom of D152. Outside the substrate-binding site, but close to D152 is a second sulphate anion that forms a hydrogen bond with the $N_{\delta 1}$ atom of H151 (SBS2). Extending further from the binding site there are two more sulphates (SBS3 and SBS4), the first interacting with the side chain atoms of R153 and N201, and the second forms a hydrogen bond with the N_{ε} of W458 from a neighbouring monomer. These SBSs represent novel binding sites which may be explored to generate chemical feature-based pharmacophore models of the binding site of this enzyme since the SBSs are located at generally conserved positions, overlapping the active site (Figure 1B).

In an effort to discover novel, non-carbohydrate inhibitors of influenza virus neuraminidase we hypothesized that compounds which contain sulphonate groups in appropriate positions, able to occupy the SBSs, might be bound tightly by the enzyme. A well-known polysulphonate molecule that acts as an inhibitor for several enzymes and proteins is Cibacron Blue 3GA (CB3GA, compound 4, Figure 2). CB3GA has been engaged in biochemical and enzymological [33] studies, and in protein purification [34]. It has been well established that CB3GA tends to bind preferentially to the active-site regions of globular proteins and mimic the binding of the naturally occurring anionic substrates and coenzymes such as NADH, ATP, coenzyme A,

flavins, and folate [21,22,25,35]. The specific interaction of sulphonic groups with protonated amino acid residues (Arg, His, Lys) on the biomolecules has been recently investigated by Friess and Zenobi [36], who have shown that the charged part of CB3GA (sulphonic groups) binds preferentially to protonated amino acid residues (Arg, His, Lys) on the biomolecules to form noncovalent complexes, whereas other sulphonates of simpler structure, such as naphthalene-sulphonic acid derivatives and 1-anilino-naphthalene-8-sulphonic acid, were found to bind preferentially to Arg. The present study was undertaken to determine whether sulphonate molecules [(e.g. CB3GA and its fragments (compounds 1-5, Figure 2)] are able to occupy the SBSs and inhibit NA, with the potential that it may lead to a new family of sulphonate-substituted affinity ligands.

Investigation of the interaction of NA with CB3GA and its fragments by difference spectroscopy and kinetic inhibition studies.

The interaction of CB3GA (compound 4, Figure 2) with NA was assessed by difference spectroscopy in the 750-500 nm region by studying the perturbation of the absorption spectrum of this compound. In the presence of NA the absorption spectrum of the dye undergoes a red shift, producing difference spectra consisting of positive maximum at the 675 nm region. Figure 3A depicts original difference spectra. CB3GA displays two broad peaks (a 675 nm positive and a 590 nm negative) and an isosbestic point at 630 nm, following a shift from its original absorbance maximum (612 nm). The shape and the wavelengths that correspond to maximum and minimum of the dye spectrum remained unchanged during titration experiments; furthermore, no time-dependent changes of absorbance were observed. These findings indicate no irreversible binding of dye to NA, and formation of a single type of complex. The increase in the extinction at positive maximum after each addition of the dye exhibits a hyperbolic dependence on the concentration of dye, indicating the formation of dye·NA complex (Figure 3B). This phenomenon was useful for the calculation of K_D of the dye·NA complexes. The results showed that NA interacts with CB3GA with high affinity, 2.1±0.2 μM (Table 1).

Subramanian [35] has shown that the shape of the spectrum describing the dye-enzyme complex is characteristic of the nature of interaction. The difference spectra

of the CB3GA, in a high salt environment, is characterized by positive maximum (690 nm) and negative double minima (630 and 585 nm), whereas the difference spectrum of the dye in binary aqueous solvents displayed a positive peak and a positive shoulder at approximately 655 and 610 nm, respectively, with a small negative contribution below 550 nm. From Figure 3A it therefore appears that the anthraquinone chromogen of CB3GA is probably located in a rather hydrophobic environment. This observation is further supported by the molecular modelling studies (see below).

To analyze which fragment of the CB3GA molecule is responsible or necessary for strong binding to NA the ability of structural fragments of CB3GA (compounds 1-3,5, Figure 2) to bind NA was investigated by kinetic inhibition analysis, and the results listed in Table 1. The results showed that each of the CB3GA fragments exhibits a different affinity for NA compared to the parent CB3GA. In general, all analogues are able to bind NA, however, the relative affinity of analogues differs by approximately 220-fold. The data presented on Table 2 points to the conclusion that smaller inhibitors (e.g. compound 5, the terminal fragment derived from the parent CB3GA) exhibits highest affinity for NA. The anthraquinone moiety (compound 1) seems not to contribute significantly to the binding affinity.

Localization of CB3GA binding site by photoaffinity labelling experiments.

Inactivation of NA by azido-CB3GA.

To characterize and locate precisely the CB3GA-binding site of NA affinity labelling experiments were performed. Affinity labelling is a useful tool for the identification and probing of specific, catalytic and regulatory sites in purified enzymes and proteins [37,38]. In the present study a new photoactive derivative of CB3GA (azido-CB3GA, Figure 4A) was synthesized and evaluated for its ability to react covalently with NA.

NA in the presence of azido-CB3GA is inactivated by irradiation. Figure 4B illustrates the decrease in the enzyme activity as a function of time of irradiation. As controls, incubation of enzyme with azido-CB3GA in the dark, or irradiation of the enzyme under the same conditions but without the reagent, caused no significant loss of enzyme activity. These results show that loss of enzyme activity was due to the reaction of enzyme and photoactivated reagent. The rate of inactivation under these

conditions was determined to be 0.017±0.002 min^{-1}. The inactivation of NA by azido-CB3GA was irreversible and enzyme activity could not be recovered by extensive dialysis nor after gel-filtration chromatography on Sephadex G-25 column in the presence or absence of 8M urea.

To determine the stoichiometry of dye binding to NA, NA was completely inactivated by the dye and the dye-enzyme covalent complex was resolved from free dye by gel filtration on Sephadex G-25 and ultrafiltration. The molar ratio of [Dye]/[NA active site] was determined by measuring the dye spectrophotometrically in urea solution, and the protein by the method of Lowry *et al.* [28]. The molar ratio of dye to NA active site was 0.94±0.15, using a subunit molecular weight 51.7 kDa, showing that the dye reacts stoichiometrically with the enzyme and therefore indicates a specific interaction between dye and protein.

The ability of specific ligands (e.g. substrates and inhibitors) to prevent enzyme inactivation by an irreversible inhibitor is the usual criterion used in arguing for binding site-directed modification [21,22,25,37,38]. Figure 4B shows that the rate of enzyme inactivation by azido-CB3GA decreased in the presence of 1 mM Neu5Ac, indicating that the dye interacts with the enzyme at the substrate-binding site.

Isolation and analysis of peptides from NA modified by azido-CB3GA.

Modified NA was subjected to chymotrypsin digestion followed by fractionation on a reverse-phase HPLC column. Essentially, a single red peak (azido-CB3GA-labelled peptide) was eluted from the column. The red peak was freeze-dried and subjected to amino acid analysis and sequencing. The overall recovery of modified peptide, based on the initial amount of modified enzyme was 36%. Edman sequence analysis of the labelled peptide gave the sequence EECSCYPDTGTVMCVC*X*DNW, where *X* indicates that no phenylthiohydantoin derivative was detected in the cycle. By comparison with the amino acid sequence of NA, the *X* in the peptide was identified as R294, indicating that the side chain of R294 is the group responsible for reacting with the azido group of the dye.

Mapping of the CB3GA binding site by molecular modelling studies.

Biochemical Journal Immediate Publication. Published on 16 Jun 2006 as manuscript BJ20060447

Molecular modelling studies were employed to provide a detailed picture of CB3GA interaction with NA. CB3GA was docked to the active site of NA with its three sulphate groups located in SBSs 1, 2 and 3. In addition to the interactions of the sulphate groups with the protein mentioned above for the individual sulphate groups, the anthraquinone moiety makes hydrophobic contacts with the aliphatic atoms of the side chains of A248, T249 and N348. The final geometry of the ligand bound is presented in Figure 5. The data listed in Table 1 and the results from molecular modelling studies suggests that the binding of CB3GA and its fragments to NA may be primarily achieved by the sulphonate moieties that provide the driving force for positioning and recognition of the analogues. This conclusion is also supported by the crystal structures of CB3GA-horse liver alcohol dehydrogenase [39] and CB3GA-glutathione S-transferase complexes [40]. The interaction of sulphonate groups of CB3GA with an arginine has been observed by Biellmann *et al*. [39]. Lowe *et al*. have used these data to investigate the interaction of CB3GA and ADH in more detail [41]: they found that different parts in the molecular structure of CB3GA exhibited completely different reactivities, except for two of the sulphonate groups. The terminal sulphonate group as well as the sulphonate group in the linking diaminobenzene-unit were found to always interact with two arginine residues of ADH. Later, Burton and coworkers [42] considered the role of the third sulphonate group bound to the anthraquinone-system. Too close proximity to the amino group inhibits a strong sulphonate dye-protein interaction. Burton also demonstrated the strong affinity of sulphonates to positively charged guanidino groups; almost no affinity between dye and protein remained after substitution of the guanidino- with a trimethylammonium-group. In the case of the CB3GA-glutathione S-transferase complex the sulphonic group linked on the anthraquinone ring interacts with the guanidyl group of R13 [40]. In the model of CB3GA docked to NA the distance between the anthraquinone amine and R294 is 3.4 Å. Thus, replacement of this amine with an azide would place the azide in close proximity to R294, in agreement with the photoaffinity labelling experiments that identified R294 as the reactive species.

Analysis of NA inhibition by benzyl-sulphonate analogues.

To analyze the contribution of the sulphonic group orientation (e.g. ortho-, meta-, para) in compound 5, two additional analogues were synthesized and their inhibitory activity was evaluated for NA using kinetic analysis. The inhibition constants (K_i)

obtained are summarized in Table 1. All analogues exhibited a competitive-type of inhibition with respect to substrate, indicating that the analogues bind at the substrate-binding site of NA. Substitution on the triazine ring for 3-aminobenzyl-sulphonic acid led to compound 6 (Figure 2) which exhibits higher affinity compared to compound 5. On the other hand, the isomer bearing bis-substituted 4-aminobenzyl-sulphonic acid (compound 7) clearly displayed a higher K_i value corresponding to about 132-fold reduction in affinity compared to compound 6. The importance of the presence of sulphonic group in the analogues was demonstrated by the compounds 8 and 9. For example, compound 8 with a single sulphonic group displays reduced affinity for NA compared to 6, whereas compound 9 lacking both sulphonic groups did not show any appreciable binding to NA.

Molecular modelling studies were also employed to provide a detailed picture of the interaction of compounds 5, 6 and 7 with NA. The analogues were docked with the sulphonic groups occupying SBSs 1 and 2 (Figure 6), consistent with their ability to inhibit competitively. This mode of binding differs from that predicted for CB3GA (Figure 5) in which the sulphonic groups of the bis-benzylsulphonate-triazine moiety bind SBSs 2 and 3. The chlorine of compound 7, although largely solvent-exposed, interacts with the hydrophobic pocket occupied by the anthraquionone of CB3GA. The chlorines of compounds 5 and 6, however, occupy a hydrophobic region that does not directly participate in binding substrate. The results from the inhibition studies (Table 1) in combination with the molecular modelling studies allow us to speculate on the origins of binding of sulphonic acid analogues to NA. The positioning of the analogues with NA may be primarily achieved by ionic interactions of the sulphonate moiety with the side chain guanidinium groups of the arginine residues 119, 294 and 372 (subsite AS1). These interactions may provide the driving force for positioning and recognition of the analogues. This is in line with the observation that compound 8, with a single sulphonic group, displays good affinity for NA, whereas compound 9, lacking both sulphonic groups, does not show any appreciable binding to NA. Compounds possessing two sulphonate groups will have a greater affinity than those with one or no sulphonate. Further support may be obtained from the recent work of Friess and Zenobi [36], who employed Matrix Assisted Laser Desorption/Ionization (MALDI) Mass Spectrometry, to demonstrate that sulphonic acid derivatives bind to arginine with higher selectivity compared to other basic sites (e.g. lysine and

histidine) of proteins. The high selectivity of sulphonate compounds for arginine is not fully understood. The principal arginine-sulphonate interaction is electrostatic in nature (a salt bridge), enhanced by ionic-hydrogen bonds that are especially favourable because of the near-perfect shape complementary of the two bidentate binding partners [36].

CONCLUSIONS

The polysulphonate molecule CB3GA and several of it structural components were shown to bind to NA. Difference spectroscopy analysis indicated that these compounds bound reversibly to the substrate binding site. CB3GA binds NA with high affinity, 2.1 μM; a derivative lacking the anthraquinone moiety binds with K_i of 0.13 μM.

Docking studies of CB3GA to NA confirmed high structural complementarity between the sulphate binding sites observed in the X-ray crystal structure and the sulphonates of the inhibitor. The anthraquinone component of the molecule was predicted to contact several hydrophobic residues on the rim of the active-site pocket, which was supported by the difference spectroscopy analysis. An azido derivative of CB3GA was shown to specifically covalently bind an active-site arginine residue in excellent agreement with the predicted conformation of CB3GA with NA.

The concept of selective staining by dyes of animal tissue and microbial organisms by Ehrlich lay the foundations of present-day chemotherapy. During the 1960's, CIBA introduced the Cibacron range of dyes, which have found utility not only as dyes but also in biomedical research. Although CB3GA and its structural components exhibit wide specificity [21,35,39], they provide access to lead structures towards the development of non-carbohydrate inhibitors to influenza NA.

REFERENCES

1. Nicholls, H. (2006) Pandemic influenza: the inside story. PLoS Biol. 4, e50.

2. Palese, P., Tumpey, T.M., Garcia-Sastre, A. (2006) What can we learn from reconstructing the extinct 1918 pandemic influenza virus? Immunity. 24, 121-124.

3. Nicholson, K.G., Wood, J. and Zambon, M. (2003) Influenza. Lancet 362, 1733-1745.

4. Colman, P.M. (1994) Influenza virus neuraminidase: structure, antibodies and inhibitors. Protein Sci. 3, 1687–1696.

5. Ward, C.W. (1981) Structure of the influenza virus hemagglutinin. Curr. Top. Microbiol. Immunol. 94-95, 1–74.

6. Palese, P., Tobita, K., Ueda, M. and Compans, R.W. (1974) Characterization of temperature sensitive influenza virus mutants defective in neuraminidase.Virology, 61, 397–410.

7. Murti, K.G., and Webster, R.G. (1986) Distribution of hemagglutinin and neuraminidase on influenza virions as revealed by immunoelectron microscopy. Virology 149, 36–43.

8. Chand, P., Babu, Y.S., Bantia, S., Chu, N., Cole, L.B., Kotian, P.L., Laver, W.G., Montgomery, J.A., Pathak, V.P., Petty, V.P., Shrout, D.P., Walsh, D.A. and Walsh, G.M. (1997) Design and synthesis of benzoic acid derivatives as influenza neuraminidase inhibitors using structure-based drug design. J. Med. Chem., 40, 4030-4052.

9. Smith, B.J., McKimm-Breshkin, J.L., McDonald, M., Fernley, R. T., Varghese, J. N and Colman, P.M. (2002) Structural studies of the resistance of influenza virus neuraminidase to inhibitors. J. Med. Chem 45, 2207-2212.

10. Smith, P.W., Sollis, S.L., Howes, P.D., Cherry, P.C., Starkey, I.D., Cobley, K.N., Weston, H., Scicinski, J., Meritt, A., Whittington, A., Wyatt, P., Taylor, N., Green, D., Bethell, R., Madar, S., Fenton, R.J., Morley, P.J., Pateman, T. and Beresford, A. (1998) Dihydropyrancarboxamides Related to Zanamivir: A New Series of Inhibitors of Influenza Virus Sialidases. 1. Discovery, synthesis, biological activity, and structure-activity relationships of 4-Guanidino- and 4-Amino-4H-pyran-6-carboxamides. J. Med. Chem. 41, 787-797.

11. Maring, C.J., Stoll, V.S., Zhao, C., Sun, M., Krueger, A.C., Stewart, K.D., Madigan, D.L., Kati, W.M., Xu, Y., Carrick, R.J., Montgomery, D.A., Kempf-Grote, A., Marsh, K.C., Molla, A., Steffy, K.R., Sham, H.L., Laver, W.G., Gu, Y.G., Kempf, D.J., Kohlbrenner, W.E. (2005) Structure-based characterization and optimization of novel hydrophobic binding interactions in a series of pyrrolidine influenza neuraminidase inhibitors. J. Med. Chem. 48, 3980-3990.

12. Macdonald, S.J., Cameron, R., Demaine, D.A., Fenton, R.J., Foster, G., Gower, D., Hamblin, J.N., Hamilton, S., Hart, G.J., Hill, A.P., Inglis, G.G., Jin, B., Jones, H.T., McConnell, D.B., McKimm-Breschkin, J., Mills, G., Nguyen, V., Owens, I.J., Parry, N., Shanahan, S.E., Smith, D., Watson, K.G., Wu, W.Y., Tucker, S.P. (2005) Dimeric zanamivir conjugates with various linking groups are potent, long-lasting inhibitors of influenza neuraminidase including H5N1 avian influenza. J. Med. Chem. 48, 2964-71.

13. Wang, G.T., Wang, S., Gentles, R., Sowin, T., Maring, C.J., Kempf, D.J., Kati, W.M., Stoll, V., Stewart, K.D., Laver, G. (2005) Design, synthesis, and structural analysis of inhibitors of influenza neuraminidase containing a 2,3-disubstituted tetrahydrofuran-5-carboxylic acid core. Bioorg. Med. Chem. Lett. 15, 125-8.

14. Blundell, T.L. (1996) Structure-based drug design. Nature 384S, 23–26.

15. Hardy, L.W. and Malikayil, A. (2003) The impact of structure-guided drug design on clinical agents. Current Drug Discovery 3, 15–20.

16. Varghese, J.N. and Colman, P.M. (1991) Three-dimensional structure of theneuraminidase of influenza virus A/Tokyo/3/67 at 2.2 Å resolution. J. Mol. Biol. 221, 473–486.

17. von Itzstein, M., Wu, W.-Y, Kok, G.B., Pegg, M.S., Dyson, J.C., Jin, B., VanPhan, T., Symthe, M.L., White, H.F., Oliver, S.W., Colman, P.M., Varghese, J.N., Ryan, D.M., Woods, J.M., Bethell, R.C., Hotham, V.J., Cameron. J.M. and Penn, C.R. (1993) Rational design of potent sialidase-based inhibitors of influenza virus replication. Nature 363, 418–423.

18. Colman, P.M. (2005) Zanamivir: an influenza virus neuraminidase inhibitor. Expert Rev. Anti Infect. Ther. 3, 191-199.

19. Varghese, J.N. (1999) Development of neuraminidase inhibitors as anti-influenza virus drugs. Drug Develop. Res. 46,176–196.

20. Dalakouras, T., Smith, B.J., Platis, D., Cox, M.M.J. and Labrou, N.E. Development of recombinant protein-based influenza vaccine: expression and purification of H1N1 influenza virus neuraminidase (submitted for publication).

21. Labrou, N.E. and Clonis, Y.D. (1995) The interaction of *Candida boidinii* formate dehydrogenase with a new family of chimeric biomimetic dye-ligands. Arch. Biochem. Biophys. 316, 169-178.

22. Labrou, N.E., Eliopoulos, E. and Clonis, Y.D. (1996) Molecular modeling for the design of dye-ligands and their interaction with mitochondrial malate dehydrogenase. Biochem. J. 315, 695-703.

23. Schauer, R. and Nohle, U. (1986) Sialidase (neuraminidase), In: Bermeyer. HU (ed) Methods of enzymatic analysis, 2nd Edn, 195-208.

24. Bradford, M.A. (1976) A rapid and sensitive method for the quantitation of microgram quantities of protein utilizing the principle of protein-dye binding. Anal. Biochem. 72, 248-254.

25. Axarli, I.A., Rigden, D.J. and Labrou, N.E. (2004) Characterization of the ligandin site of maize glutathione S-transferase I. Biochem J. 382, 885-893.

26. Morrill, P.R., Gupta, G., Sproule, K., Winzor, D., Christensen, J., Mollerup, I., Lowe, C.R. (2002) Rational combinatorial chemistry-based selection, synthesis and evaluation of an affinity adsorbent for recombinant human clotting factor VII. J Chromatogr B Analyt Technol Biomed Life Sci. 774, 1-15.

27. Palanisamy, U.D., Winzor, D.J. and Lowe, C.R. (2000) Synthesis and evaluation of affinity adsorbents for glycoproteins: an artificial lectin. J. Chromatogr. B Biomed. Sci. Appl. 746, 265-281.

28. Lowry, O.H., Rosebrough, N.J., Farr, A.L. and Randall, R.S. (1951) Protein Measurement with the Folin Phenol Reagent. J. Biol. Chem. 193, 265-275.

29. Smith, B.J., Huyton, T., Joosten, R.P., McKimm-Breschkin, J.L., Zhang, J.-G., Luo, C. S., Lou, M.-Z., Labrou, N.E., and Garrett T.P.J. X-ray Crystal Structure of a Calcium Deficient Form of Influenza Virus Neuraminidase: Implications for Substrate Binding. Acta Crystalogr. D, (in press).

30. SYBYL 6.8 release, Tripos Inc., St. Louis, MO 63144, USA.

31. Ewing, T.J., Makino, S., Skillman, A.G. and Kuntz, I.D. (2001) DOCK 4.0: search strategies for automated molecular docking of flexible molecule databases. J. Comput. -Aided Mol. Des. 15, 411-428.

32. Meng, E.C., Shoichet, B.K. and Kuntz, I.D. (1992) Automated docking with grid-based energy evaluation. J. Comp. Chem. 13, 505-524.

33. Lyon, R.P., Hill, J.J. and Atkins, W.M. (2003) Novel class of bivalent glutathione S-transferase inhibitors. Biochemistry 42, 10418-10428.

34. Labrou, N.E. (2003) Design and selection of affinity ligands for affinity chromatography. J. Chromatogr. B, 790, 67-78.

35. Subramanian, S. (1982) Spectral changes induced in Cibacron Blue F3GA by salts, organic solvents, and polypeptides: implications for blue dye interaction with proteins. Arch. Biochem. Biophys. 216, 116-125.

36. Friess, S.D. and Zenobi, R. (2001) Protein Structure Information from Mass Spectrometry? Selective Titration of Arginine Residues by Sulfonates. J. Am. Soc. Mass Spectrom. 12, 810–818

37. Pettigrew, N.E., Brush, E.J. and Colman, R.F. (2001) 3-Methyleneoxindole: an affinity label of glutathione S-transferase pi which targets tryptophan 38. Biochemistry 40, 7549-7558.

38. Wang, J., Bauman, S. and Colman, R.F. (2000) Probing subunit interactions in alpha class rat liver glutathione S-transferase with the photoaffinity label glutathionyl S-[4 (succinimidyl)benzophenone]. J. Biol. Chem. 275, 5493-5503.

39. Biellmann, J.-F., Samama, J.-P. , Branden, C.I. and Eklund, H. (1979) X-ray studies of the binding of Cibacron blue F3GA to liver alcohol dehydrogenase. Eur. J. Biochem. 102, 107.

40. Oakley, A.J., Lo Bello, M., Nuccetelli, M., Mazzetti, A.P., and Parker, M.W. (1999) The ligandin (non-substrate) binding site of human Pi class glutathione transferase is located in the electrophile binding site (H-site). J. Mol. Biol. 291, 913-926.

41. Lowe, C.R.,. Burton, S.J Pearson, J.C., Clonis, Y.D. and Stead, V. (1986) Design and application of bio-mimetic dyes in biotechnology. J. Chromatogr. 376, 121-130.

42. Burton, S.J., Stead, C.V. and Lowe, C.R. (1990) Design and applications of biomimetic anthraquinone dyes. III. Anthraquinone-immobilised C.I. reactive blue 2

analogues and their interaction with horse liver alcohol dehydrogenase and other adenine nucleotide-binding proteins. J. Chromatogr. 508, 109-125.

Biochemical Journal Immediate Publication. Published on 16 Jun 2006 as manuscript BJ20060447

Table 1. Binding characteristics of CB3GA and its fragments to recombinant neuraminidase. The structures of analogues are depicted in Figure 2. Inhibition constants (K_i) were determined by kinetic inhibition studies.

Compound	K_i(μM)]
1	56.5±4
2	12.5±2
3	12.8±1.9
4	2.9±0.2*
5	0.28±0.04
6	0.13±0.05
7	17.1±1.9
8	4.3±0.7
9	No detectable binding

*The value of 2.1±0.2 for compound 4 was determined by difference spectra titrations.

FIGURE LEGENTS

Figure 1.

A. The sulphate binding sites SBS1-4 of NA as observed from the 2.2 Å crystal structure (PDB code 2B8H, [29]). Sulphate anions are presented as thin tubes, and the side-chains of binding residues are displayed as heavy tubes.

B. The sulphate binding residues of influenza A neuraminidases of different subtypes (N1 to N9). Amino acids that form the sulphate binding sites SBS1-4 are marked with *. The partial alignments were produced using ESPript. Abbreviations for neuraminidases are in brackets: A/Beijing/262/95 (N1) A/Chicken/California/9420/2001(N2); A/turkey/California/6878/79(N3); A/mink/Sweden/E12665/84(N4); A/shearwater/Australia/1/72 (N5); A/sanderling/Delaware/1258/86(N6); avian/FPV/Weybridge (N7); A/Turkey/Canada/63 (N8); A/whale/Maine/1/84(N9).

Figure 2.

The structure of CB3GA analogues used in the present study. 1: 1-amino-4-bromo-9,10-dioxo-4a,9,9a,10-tetrahydroanthracene-2-sulphonic acid; 2: 1-amino-4-[(4-amino-3-sulphophenyl)amino]-9,10-dioxo-4a,9,9a,10-tetrahydroanthracene-2-sulphonic acid; 3: hydrolized 1-Amino-4-[3-(4,6-dichlorotriazin-2-ylamino)-4-sulphophenylamino]anthraquinone-2-sulphonic acid, 4: Cibacron Blue 3GA; 5: 2-({4-chloro-6-[(2-sulphophenyl)amino]-1,3,5-triazin-2-yl}amino)benzenesulphonic acid; 6: 3-({4-chloro-6-[(3-sulphinophenyl)amino]-1,3,5-triazin-2-yl}amino)benzenesulphonic acid; 7: 4-({4-chloro-6-[(4-sulphophenyl)amino]-1,3,5-triazin-2-yl}amino)benzenesulphonic acid; 8: 3-[(4-anilino-6-chloro-1,3,5-triazin-2-yl)amino]benzenesulphonic acid; 9: 6-chloro-*N*,*N*'-diphenyl-1,3,5-triazine-2,4-diamine.

Figure 3.

Difference spectra titrations. A. Difference spectra of CB3GA (from top to bottom: 15, 5, 2, μM CB3GA) in the presence of recombinant neuraminidase at pH 5.9 and 37°C. **B**. The difference absorbance at 675 nm as a function of the total CB3GA concentration (2-20 μM) for NA.

Figure 4.

A. The structure of azido-CB3GA.

B. Photoaffinity labelling of neuraminidase by azido-CB3GA at pH 5.9 and 4^{o}C. Recombinant neuraminidase was incubated in the absence (filled rhomb) or in the presence of azido-CB3GA at concentration of 20 μM (filled square). At the times indicated, aliquots were withdrawn diluted and assayed for enzymatic activity. Enzyme was also incubated in the presence of 20 μM azido-CB3GA and Neu5Ac (1 mM, open square).

Figure 5.

Interaction of CB3GA with NA from docking calculations. The solvent accessible surface of the sulphate binding sites is colored blue (SBS1), red (SBS2) and green (SBS3). The sulphate ions identified in the X-ray analysis are displayed as thin rods. Side-chains of specific residues contributing to the SBSs and interacting with the ligand are presented as heavy rods beneath the transparent surface. Atoms are coloured white (H), cyan (C), blue (N), red (O), yellow (S) and grey (Cl). The sulphur atoms of the ligand coincide with the sulphate sulphur atoms. The figure was prepared using DINO (http://www.dino3d.org).

Figure 6.

Modelling of benzyl-sulphonate analogues in the active site of NA. 2-aminobenzyl-sulphonate - compound 5 (left panel); 3-aminobenzyl-sulphonate - compound 6 (middle panel); 4-aminobenzyl-sulphonate - compound 7 (right panel). Colours of the surface of NA and atoms are the same as detailed in Figure 5. The sulphate ions observed in the X-ray structure are presented as thin rods.

Biochemical Journal Immediate Publication. Published on 16 Jun 2006 as manuscript BJ20060447

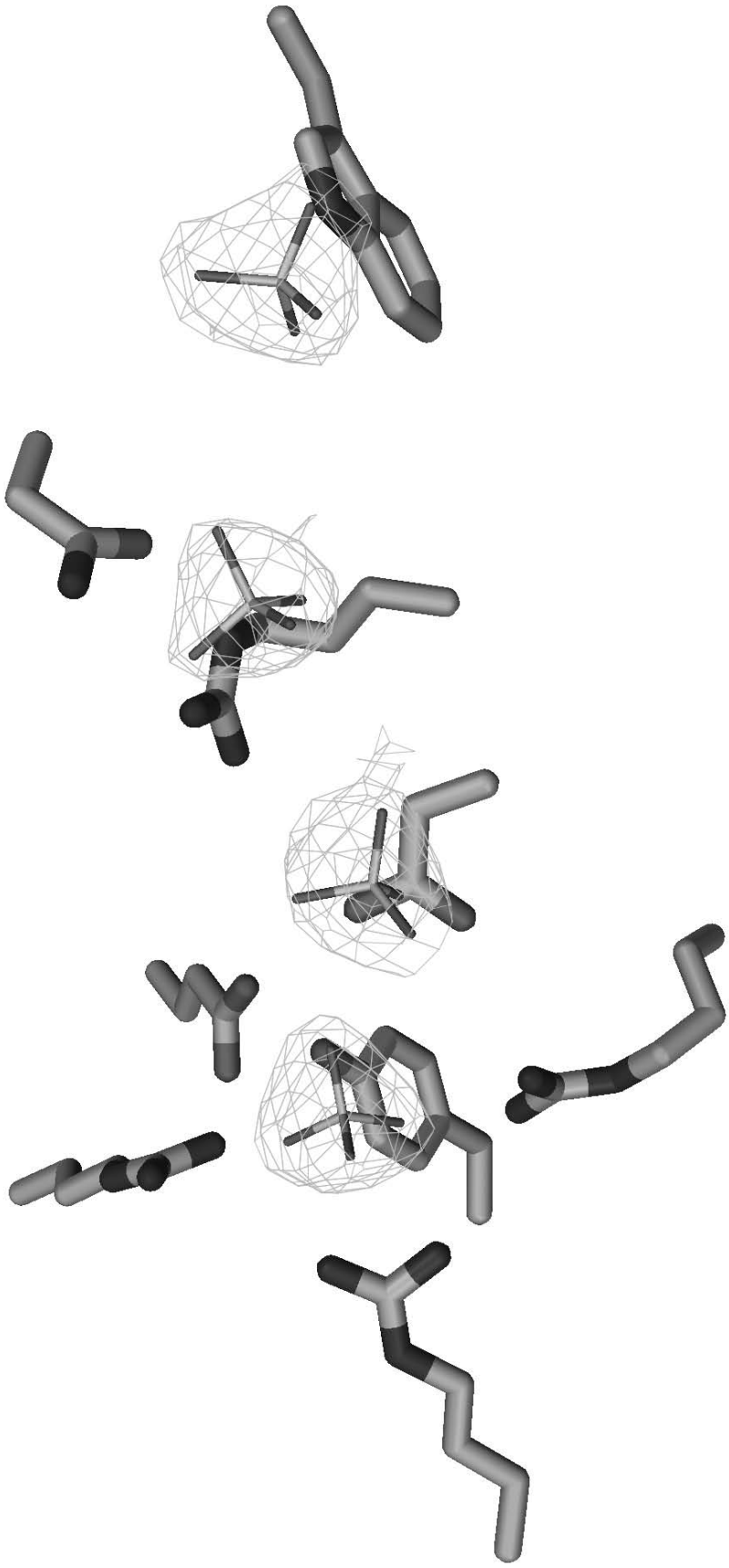

Figure 1A

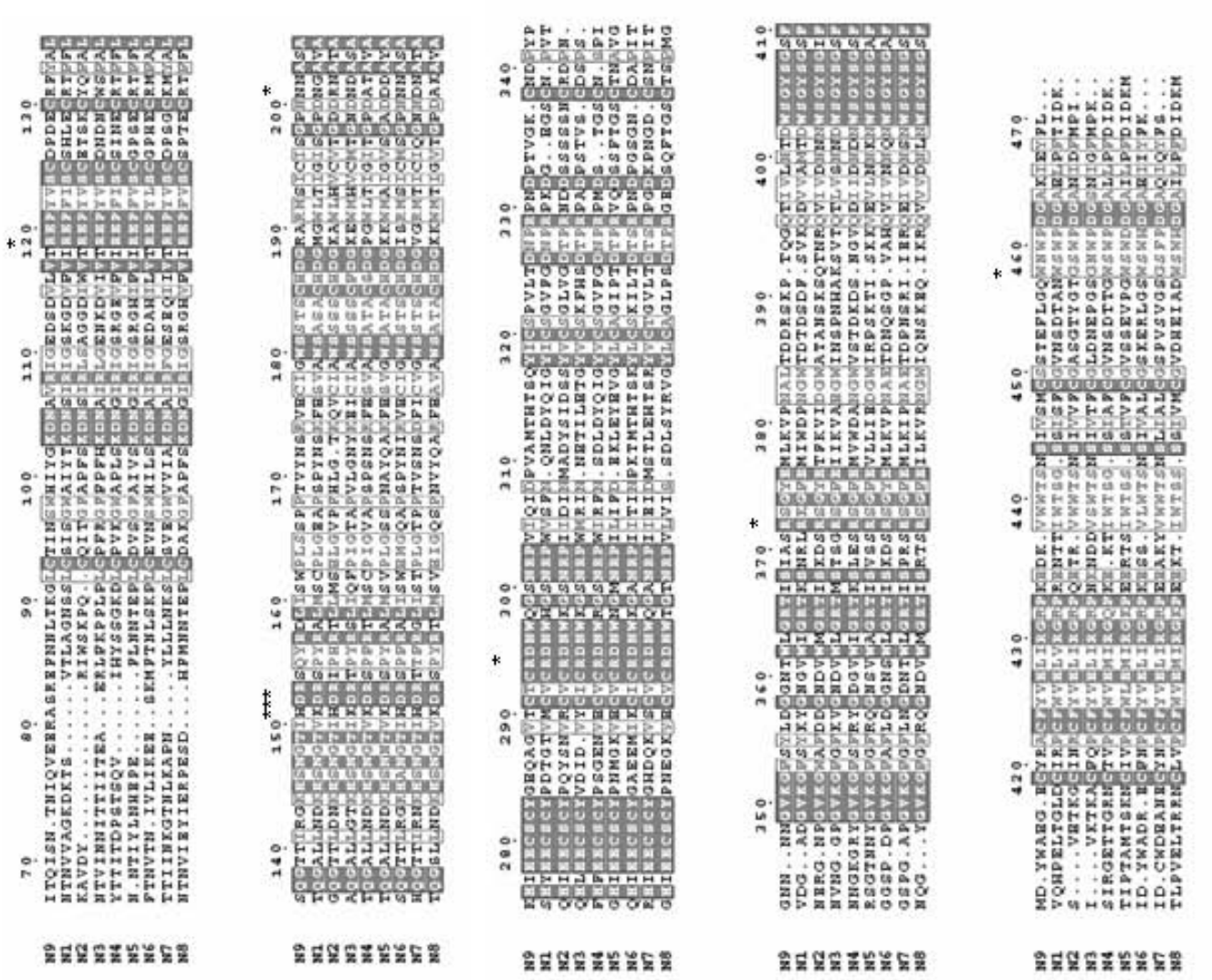

Figure 1B

Compound 1

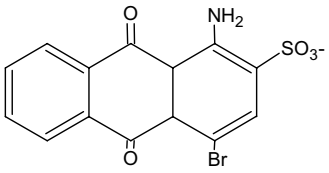

Compound 2

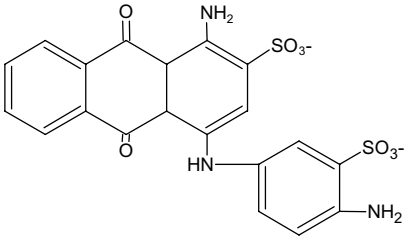

Compound 3

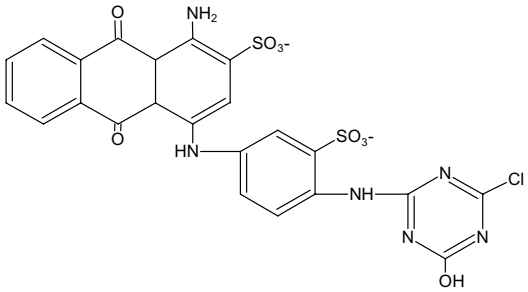

Compound 4

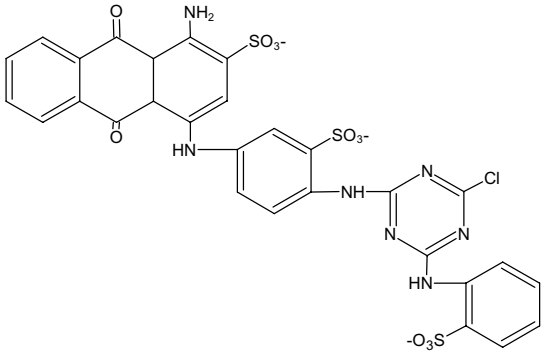

Compound 5

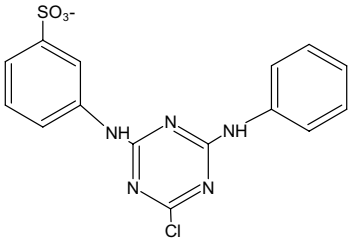

Compound 6

Compound 7

Compound 8

Compound 9

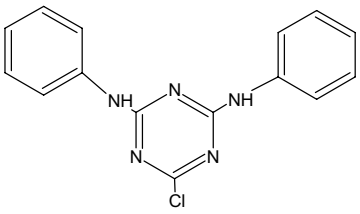

Figure 2.

Biochemical Journal Immediate Publication. Published on 16 Jun 2006 as manuscript BJ20060447

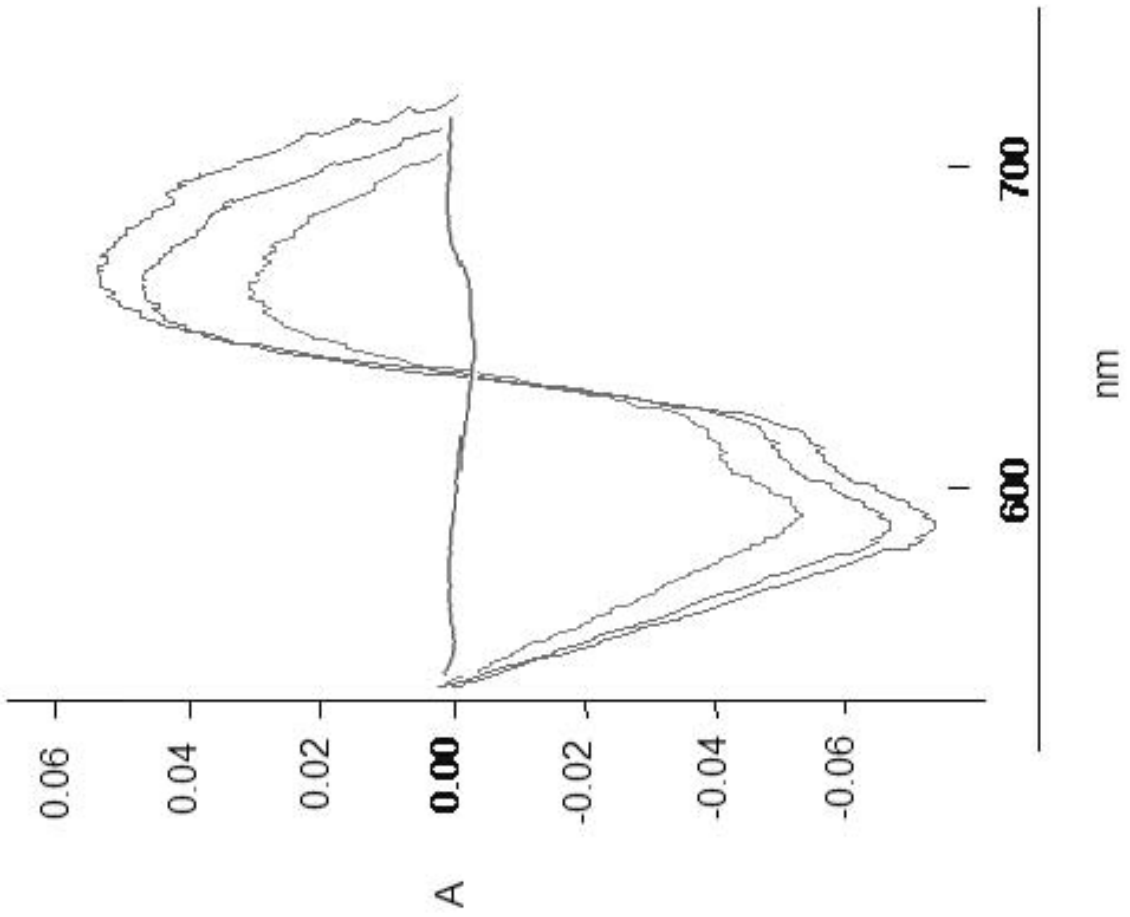

Figure 3A

Biochemical Journal Immediate Publication. Published on 16 Jun 2006 as manuscript BJ20060447

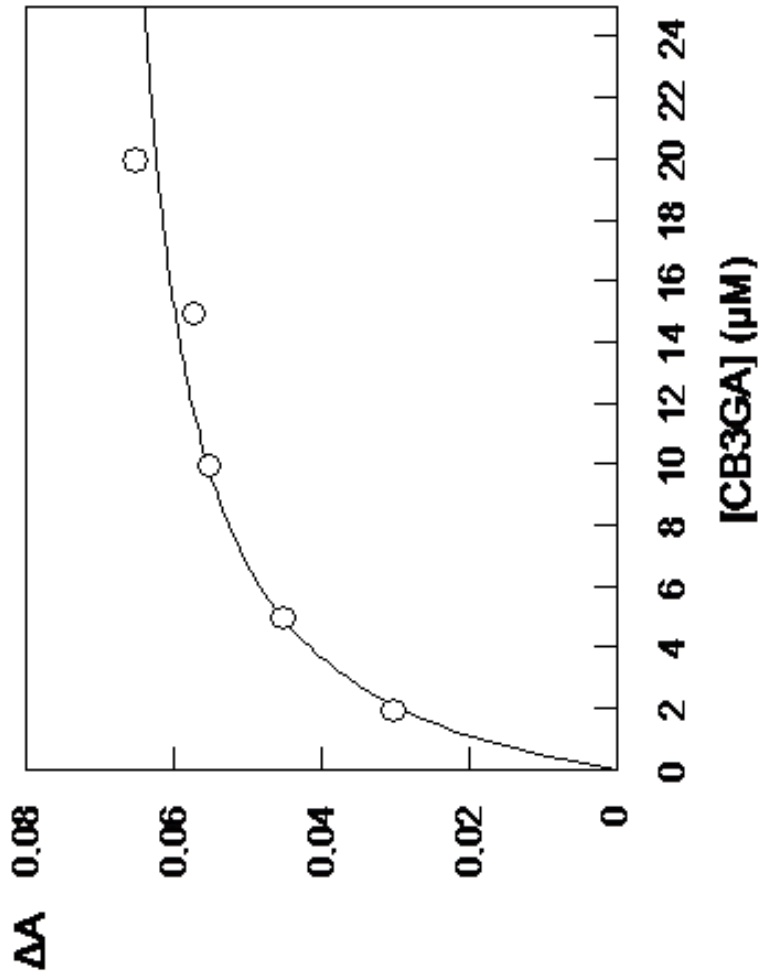

Figure 3B

Biochemical Journal Immediate Publication. Published on 16 Jun 2006 as manuscript BJ20060447

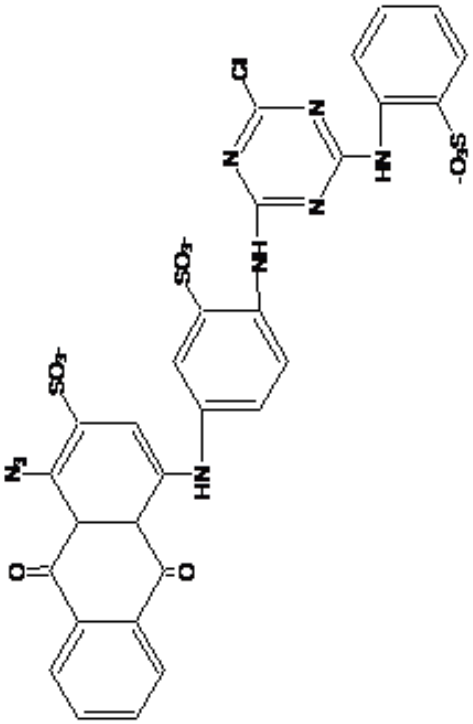

Figure 4A

Biochemical Journal Immediate Publication. Published on 16 Jun 2006 as manuscript BJ20060447

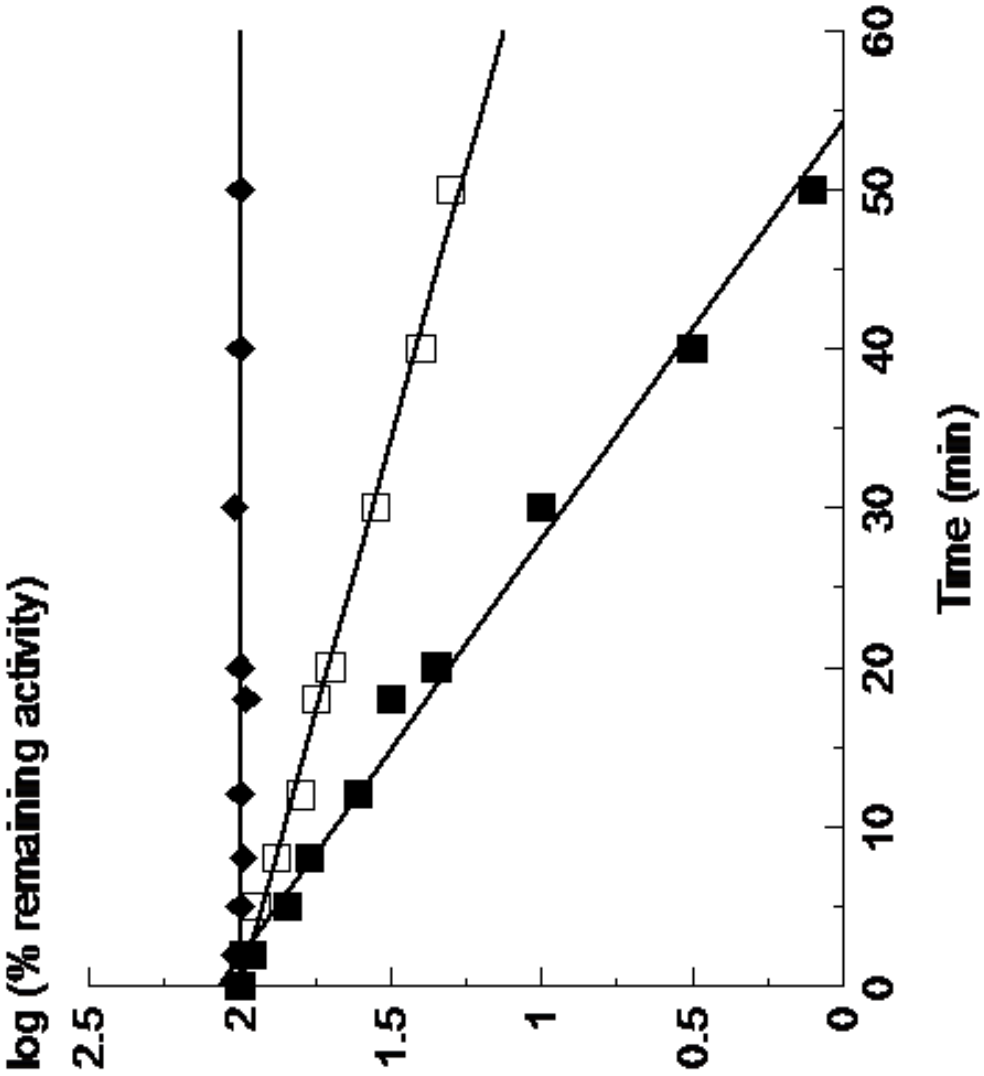

Figure 4B

Biochemical Journal Immediate Publication. Published on 16 Jun 2006 as manuscript BJ20060447

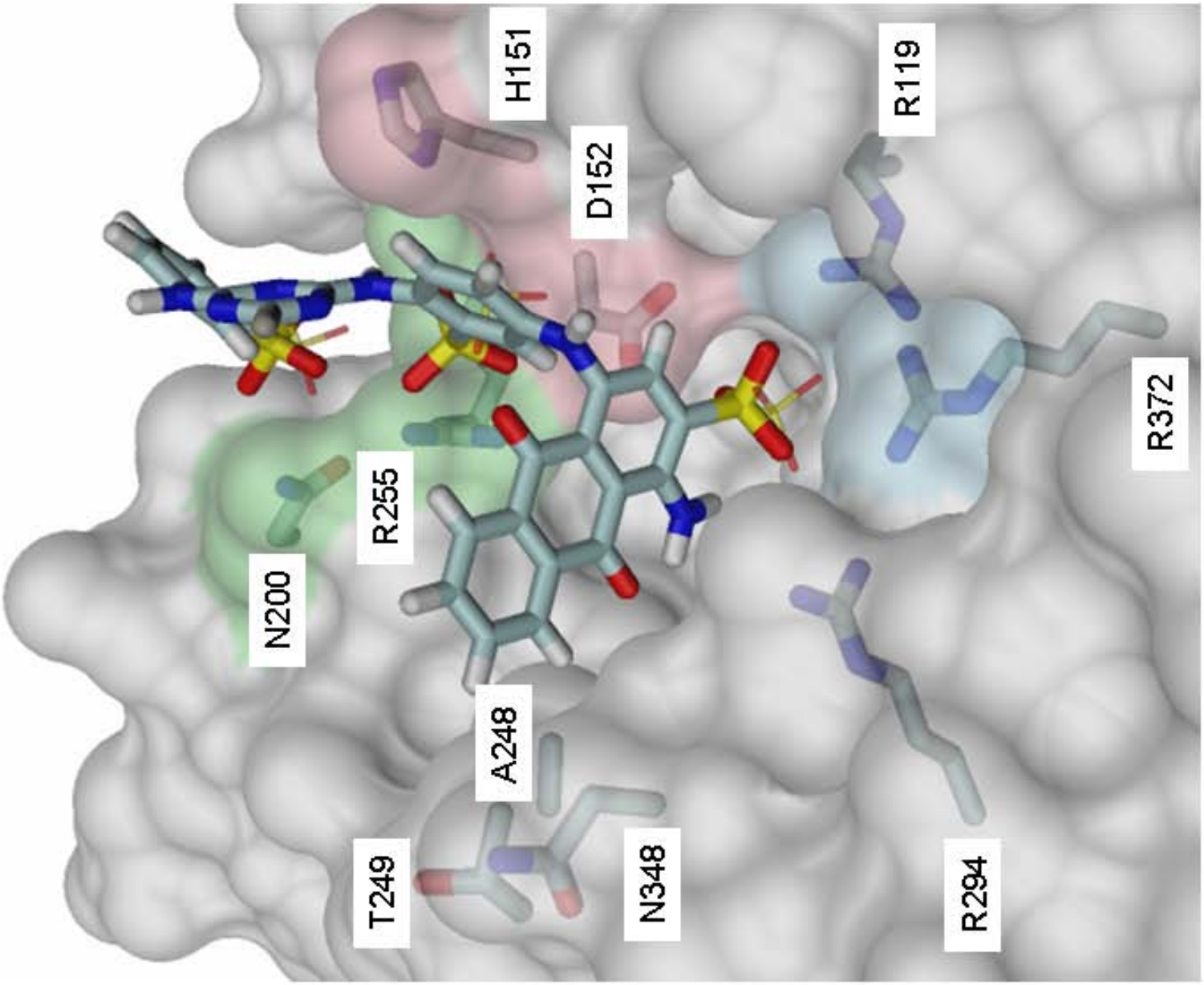

Figure 5

Biochemical Journal Immediate Publication. Published on 16 Jun 2006 as manuscript BJ20060447

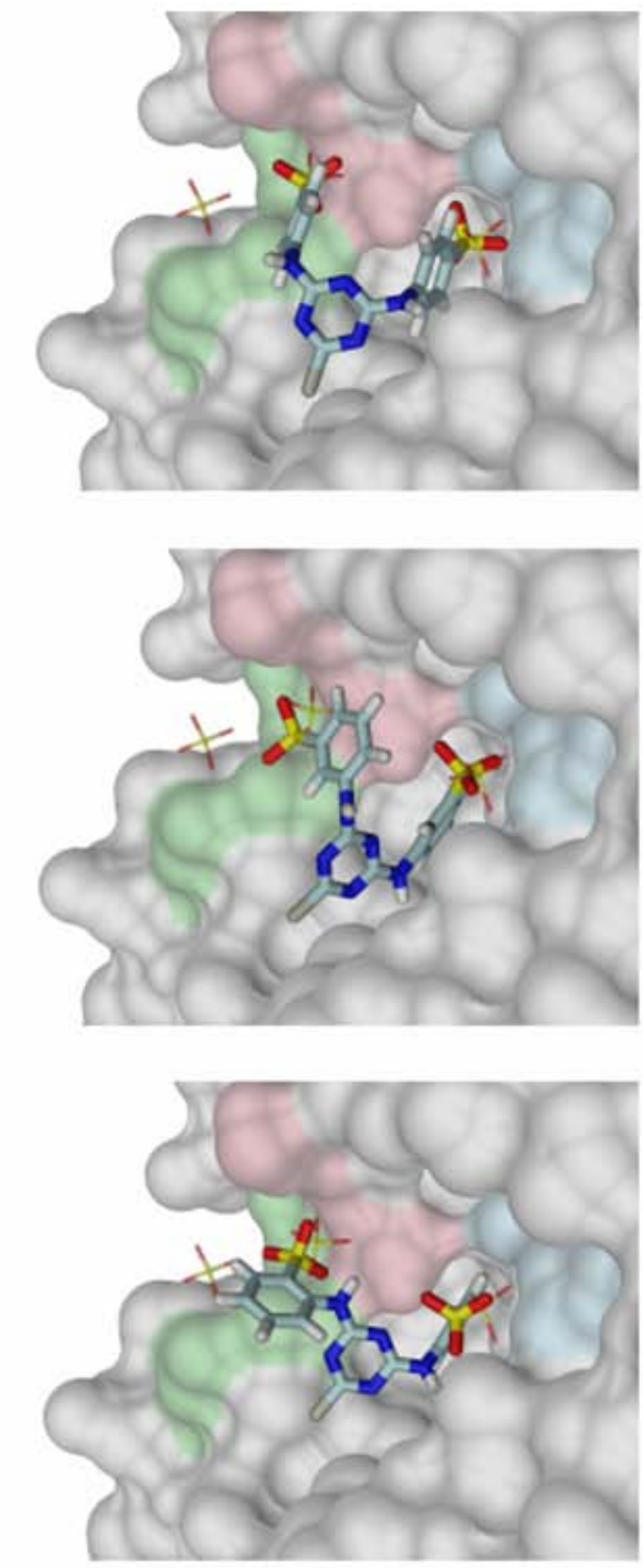

Figure 6